Structure *16*

Supplemental Data

The GTPase Cycle of the Chloroplast Import Receptors Toc33/Toc34: Implications from Monomeric and Dimeric Structures

Patrick Koenig, Mislav Oreb, Anja Höfle, Sabine Kaltofen, Karsten Rippe, Irmgard Sinning, Enrico Schleiff, and Ivo Tews

Supplemental Experimental Procedures

Calculation of the Solid Phase Binding

Equation

$$[Bound] = -\,\mathrm{sqrt}[\,(K+S+E)^2 / 4 - S*E] + (K+S+E)/2 \qquad \text{(E1)}$$

is derived from

$$K = [E]*[S]/[Bound] \qquad \text{(E3)}$$

where $[S]$ is the free concentration of spotted protein, $[E]$ the free concentration of added protein (normalized), $[Bound]$ is the concentration of complexes formed and K the dissociation constant in a not normalized situation and an apparent dissociation constant after normalization. Considering the two relations

$$[E] = E - [Bound] \qquad \text{(E4)}$$

and

$$[S] = S - [Bound] \qquad \text{(E5)}$$

where S is the total concentration of spotted protein, and E the total concentration of added protein (normalized), equation (E3) can be written as

$$K = (E - [Bound])*(\,S - [Bound])/[Bound] \qquad \text{(E1')}$$

which can be rewritten as

$$[Bound] = \pm\,\mathrm{sqrt}[\,(K+S+E)^2 / 4 - S*E] + (K+S+E)/2 \qquad \text{(E6)}$$

The decision for the negative algebraic sign in equation (E1) comes from the following simple consideration: suppose *S* is zero, then [*Bound*] must be zero as well, which satisfied with negative algebraic sign.

Calculation of the Hydrolysis Rate

The apparent rate constants determined for different concentrations of the receptor can be analysed by equation (E2) for the following reason. The hydrolysis kinetic can be analyzed by

$$FH(t,T) = D/T * (1-\exp(-k_D*t)) + (T-D)/T * (1-\exp(-k_M*t)) \quad (E7)$$

with FH fold hydrolysis, D the concentration in dimeric conformation, T the total concentration of the GTPase, k_D the rate constant of the protein in dimeric conformation and the k_M rate constant in monomeric conformation. The apparent rate constant was determined at a given concentration by

$$FH(t)= 1-\exp(-k_{app}*t) \quad (E8)$$

can be written as

$$1-\exp(-k_{app}*t) = D/T*(1-\exp(-k_D*t))+(T-D)/T*(1-\exp(-k_M*t)) \quad (E9)$$

Hence, the following three transformations lead to the relation of the apparent rate constant

$$\exp(-k_{app}*t) = 1 - (D/T*(1-\exp(-k_D*t))+(T-D)/T*(1-\exp(-k_M*t))) \; k_{app}$$

$$= - \ln(1 - (D/T*(1-\exp(-k_D*t))+(T-D)/T*(1-\exp(-k_M*t))) / t \quad (E10)$$

Using the two approximations that $\ln(1-x) \sim - x$ and $\exp(x) \sim 1+x$ (both true since $x<1$), equation (E10) can be written as

$$k_{app}= D/T * k_D + (T-D)/T * k_M \quad (E2)$$

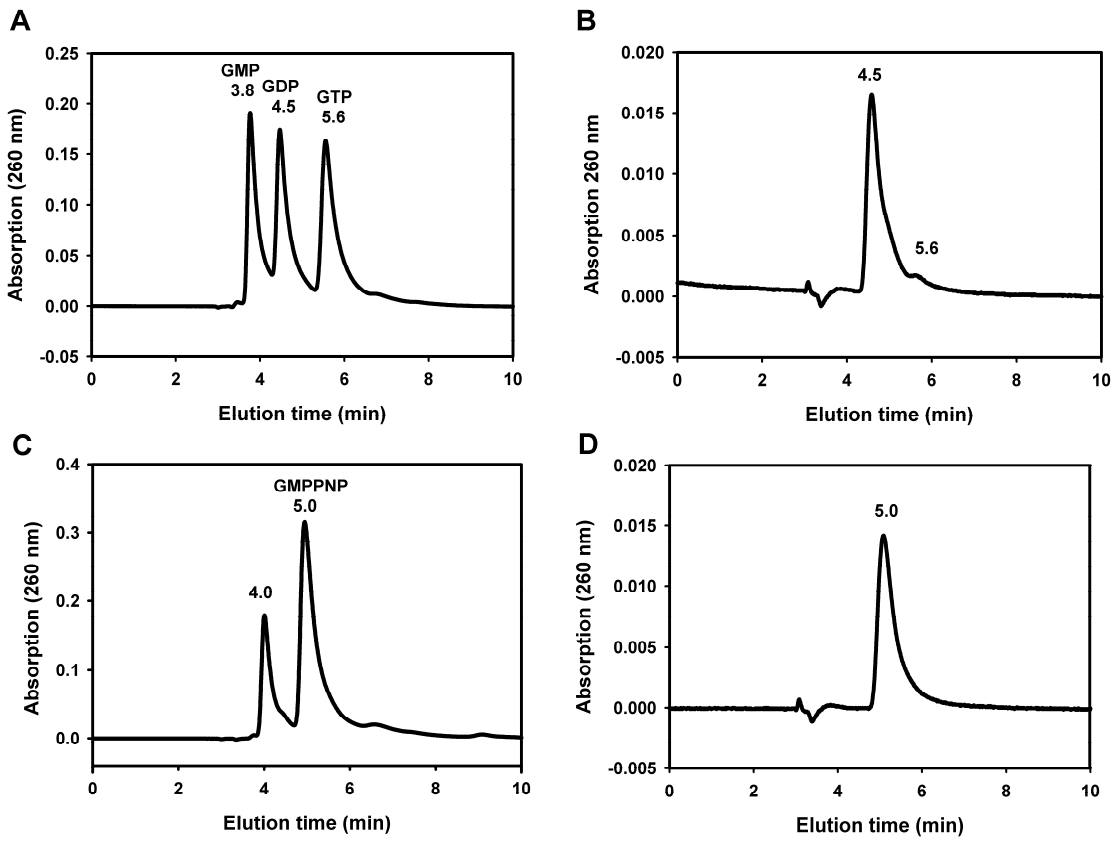

Figure S1. Nucleotide Binding State of *ps*Toc34 GTPase

(A) Elution profile of a 1 mM mixture of GMP, GDP and GTP standards. Retention times are 3.8 min, 4.5 min and 5.6 min, respectively. (B) Elution of nucleotides from freshly purified *at*Toc33, showing a mixture of GDP and GTP loaded protein. (C) Elution profile of a 1 mM GMPPNP standard. The peak observed at 5 min originates from GMPPNP, while the peak at 4.0 min represents a known impurity resulting from of the production process (GMPPNP from Sigma Aldrich has a certified purity of > 85%). (D) Elution profile of GMPPPNP loaded *at*Toc33 using the nucleotide exchange protocol. GMPPNP is detectable as a single peak at 5 min retention time; the impurity observed with the GMPPNP standard in (C) at 4 min retention time is not seen in the GMPPNP exchanged protein sample. In all experiments a volume of 20 µl of injected on the column, the protein concentration was adjusted to 50 µM, the flow rate used was 1.0 ml/min.

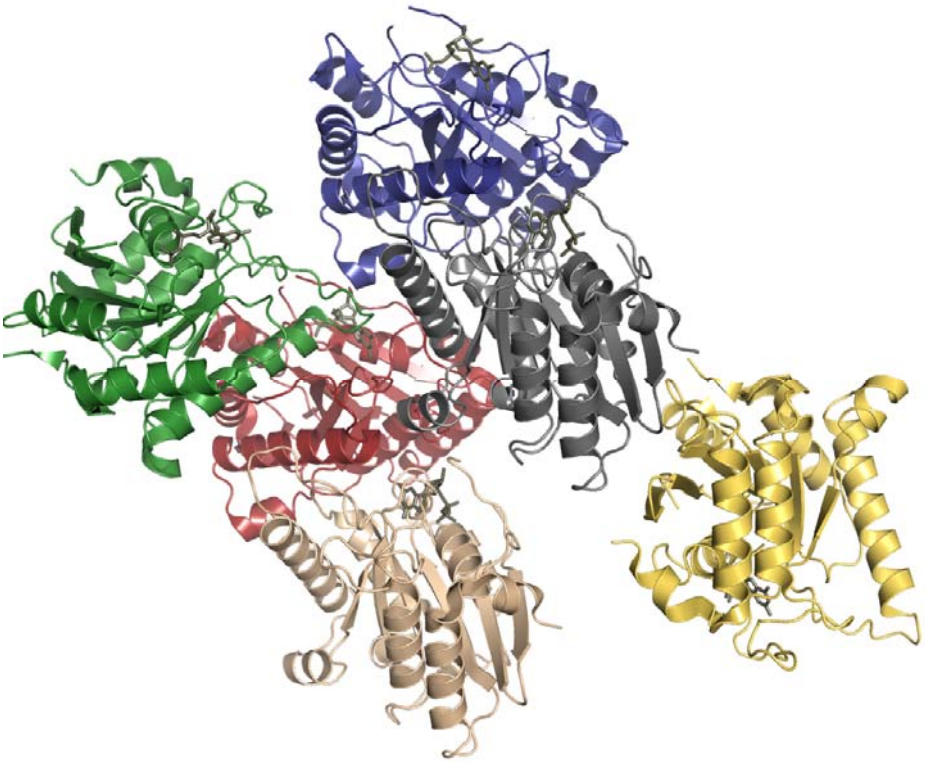

#	interacting monomer	symmetry operation	interface area [Å^2]
1	blue	-y+1/2,x+1/2,z+1/4	674.1
2	orange	y,x,-z	424.8
3	red	-y+1/2,x+1/2,z-3/4	328.5
4	brown	x,y,z-1	138.9
5	green	-x,-y+1,z-1/2	82.3

Figure S2. Analysis of Crystal Contacts
The table shows the relevant interfaces formed in the crystal between the grey monomer and neighbouring molecules, as calculated by the program PISA (Krissinel and Henrick, 2007). For comparison, the interface observed in the *ps*Toc34 dimer has a calculated interface area of 2750 Å^2.

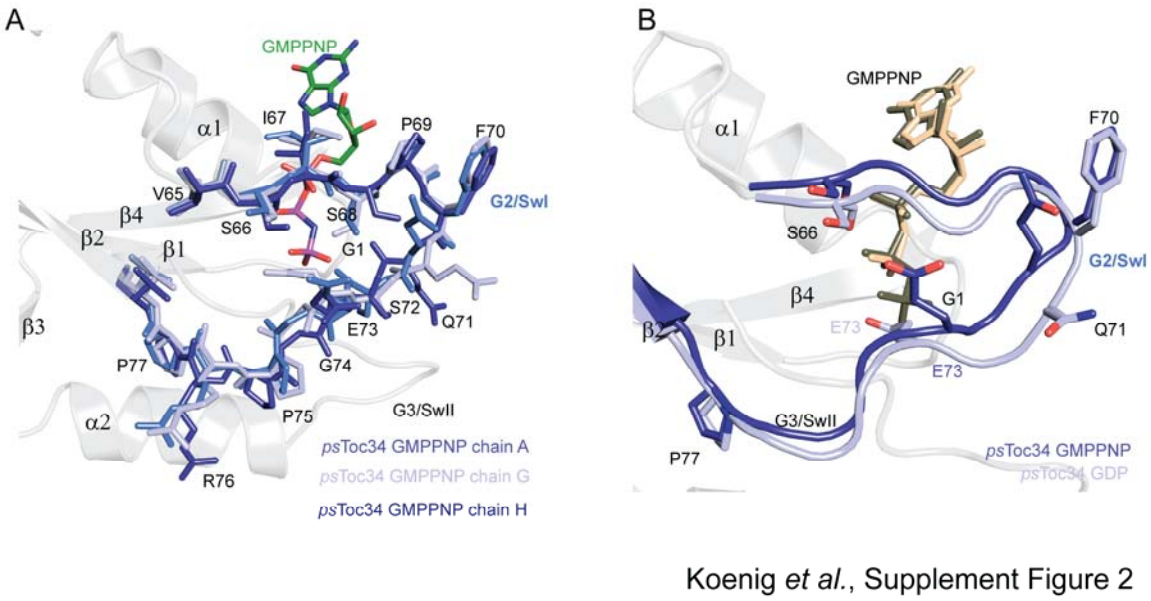

Figure S3. Disorder in the G2 / Switch I Element in Dimeric *ps*Toc34

(A) There are subtle changes in the G2 / switch I region, when the eight copies in the asymmetric unit are compared. The G2 / switch I region from Gln71 to Arg76 is somewhat flexible, though the conformational freedom is partly restricted by presence of the two prolines Pro69 and Pro75.

(B) Comparison of the G2 / switch I region between $Toc34_{GMPPNP}$ and $Toc34_{GDP}$. The main difference between GDP and GMPPNP states is positioning of Glu73 as discussed in the main text, this is the nucleotide *tracker* residue which monitors the nucleotide loading state.

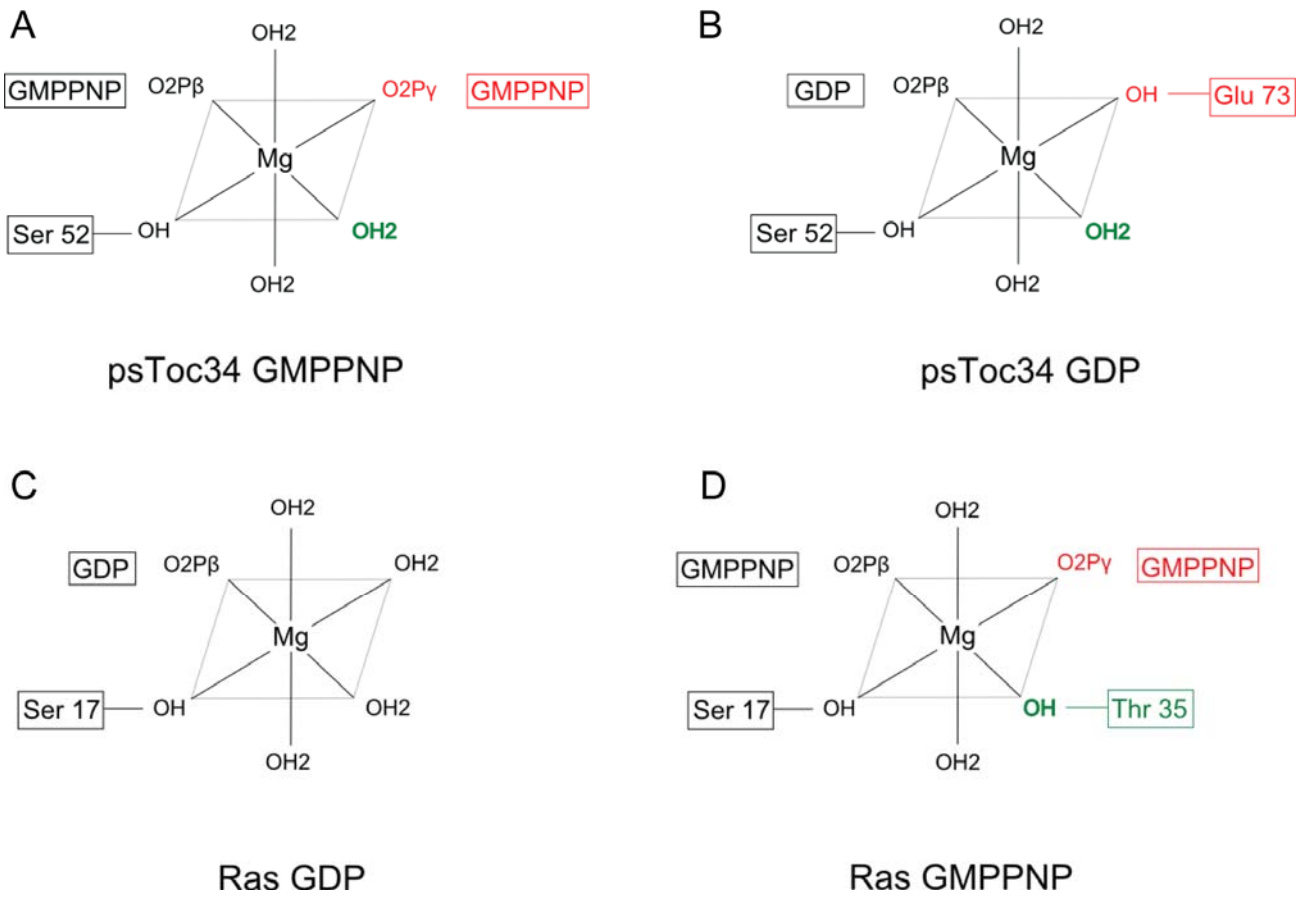

Figure S4. Mg^{2+} Coordination in *ps*Toc and p21 Ras

(A) Coordination of the magnesium-ion in the GMPPNP state of *ps*Toc34 by Ser52 from the G1 element, the β- and the γ-phosphate and three additional water molecules.

(B) Coordination of the magnesium-ion in the GDP state of *ps*Toc34 by Ser52 from the G1 element, Glu73 from the G2 element, the β-phosphate and three additional water molecules. Glu73 takes the coordination site of the γ-phosphate in $Toc34_{GMPPNP}$ as shown in (A)

(C) Coordination of the magnesium-ion in the GMPPNP state of p21 Ras. The magnesium-ion is coordinated by Ser17 from the G1 element, the β- and the γ-phosphate, a Thr from the G2 element, which is conserved among GTPases of the TRAFAC class and two additional water molecules.

(D) Coordination of the magnesium-ion in the GDP state of p21 Ras. The magnesium-ion is coordinated by Ser17 from the G1 element, the β-phosphate and three additional water molecules.

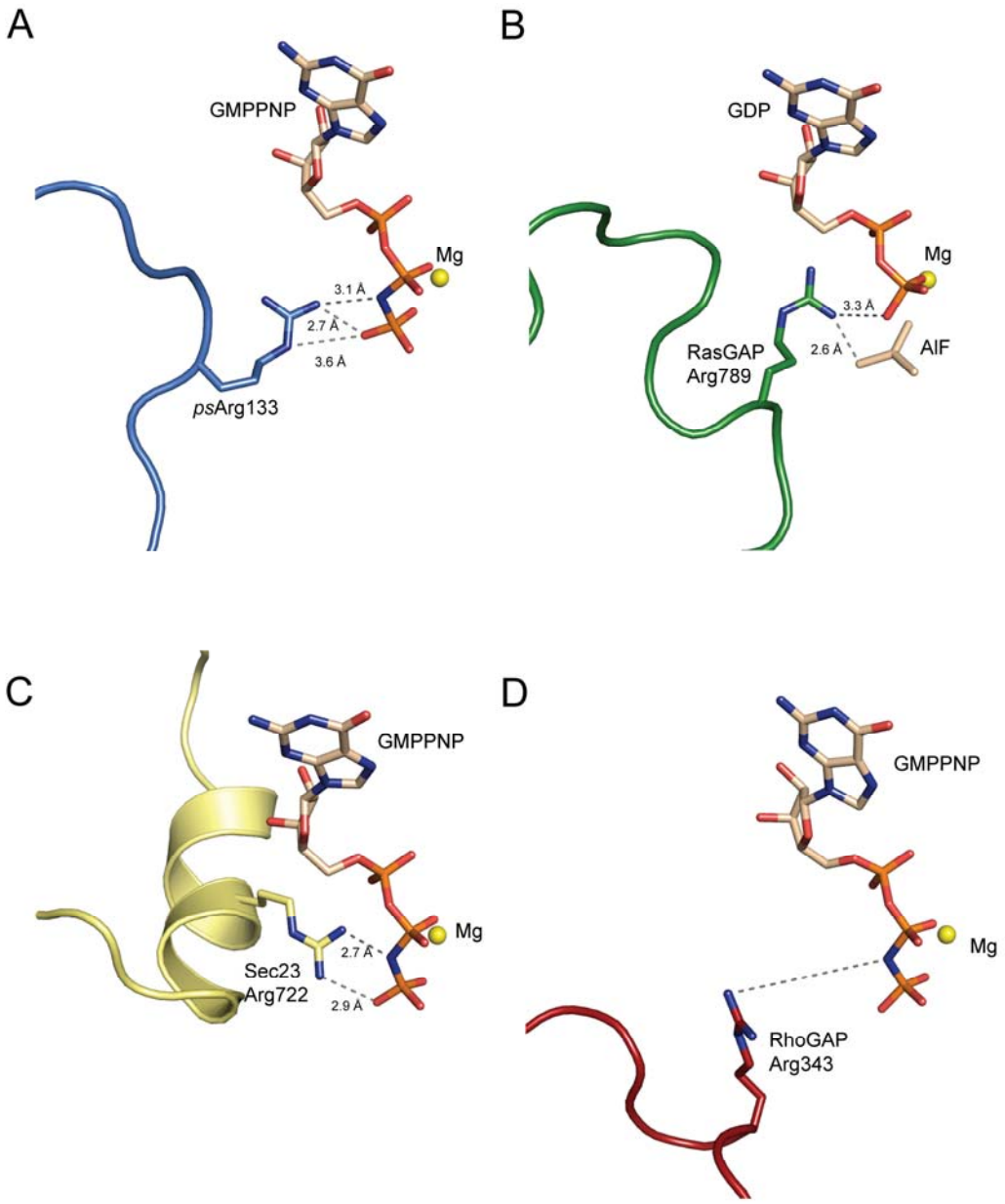

Figure S5. Comparison of *ps*Arg133 with Arginine Finger in different GTPase-GAP Complexes

(A) *ps*Toc34 CB-loop carring Arg133 inserted *in trans* in the nucleotide binding pocket of the dimerisation partner. (B) RasGAP-Ras argenine finger (PDB 1WQ1). A similar confirmation of arginine fingers is observed in the Cdc42:Cdc42GAP:GDP:AlF (PDB 1GRN) and in the Rho:RhoGAP:GDP:AlF (PDB 1TX4) structure. (C) Sec23:Sar1:GMPPNP arginine finger (PDB 1M2O). (D). Cdc42:RhoGAP GMPPNP arginine finger, which is turned away from the nucleotide and not in proper conformation for hydrolysis activation (PDB 1AM4).

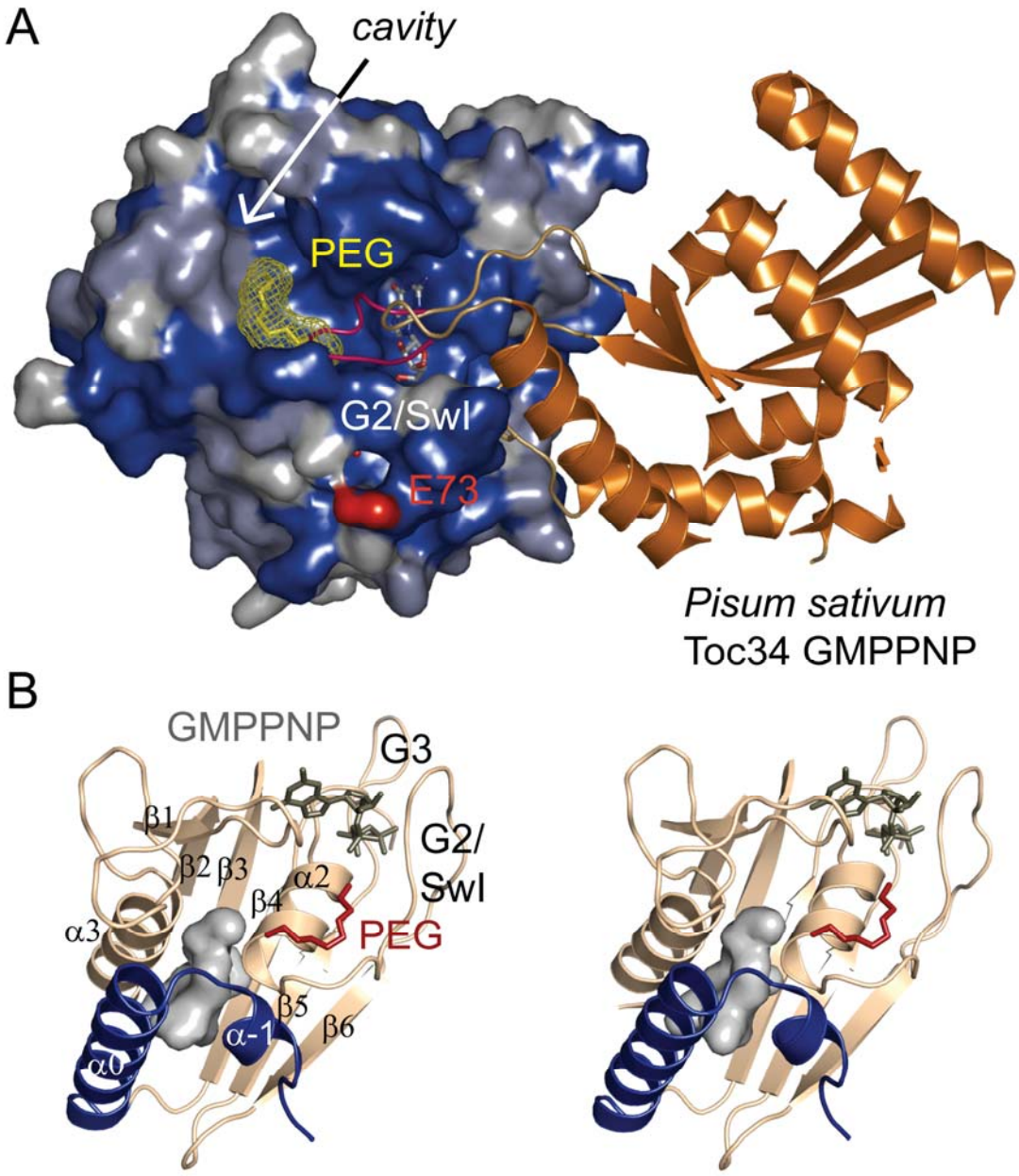

Figure S6. Binding Sites on Toc34

(A) Surface of Toc34 colored by the degree of conservation. Conservation is based on the alignment shown in Figure S7, using the program Consurf (Glaser et al., 2003). Dark colors show highly conserved residues, light colors variable regions. The regions around the potential binding site are highly conserved. Model of Toc159 as well as E73 compare Figure 6. (B) A PEG molecule is bound at a shallow cavity on the surface of *ps*Toc34. This molecule, originating from the crystallization conditions, binds close to the G2 elements and thus is in a suggestive position for an interaction that would occur in the Toc complex. Near the PEG binding site, there is a large cavity between helix α-1 and helix α0 and the central β-sheet of the GTPase domain. The cavity might be also part of the binding site.

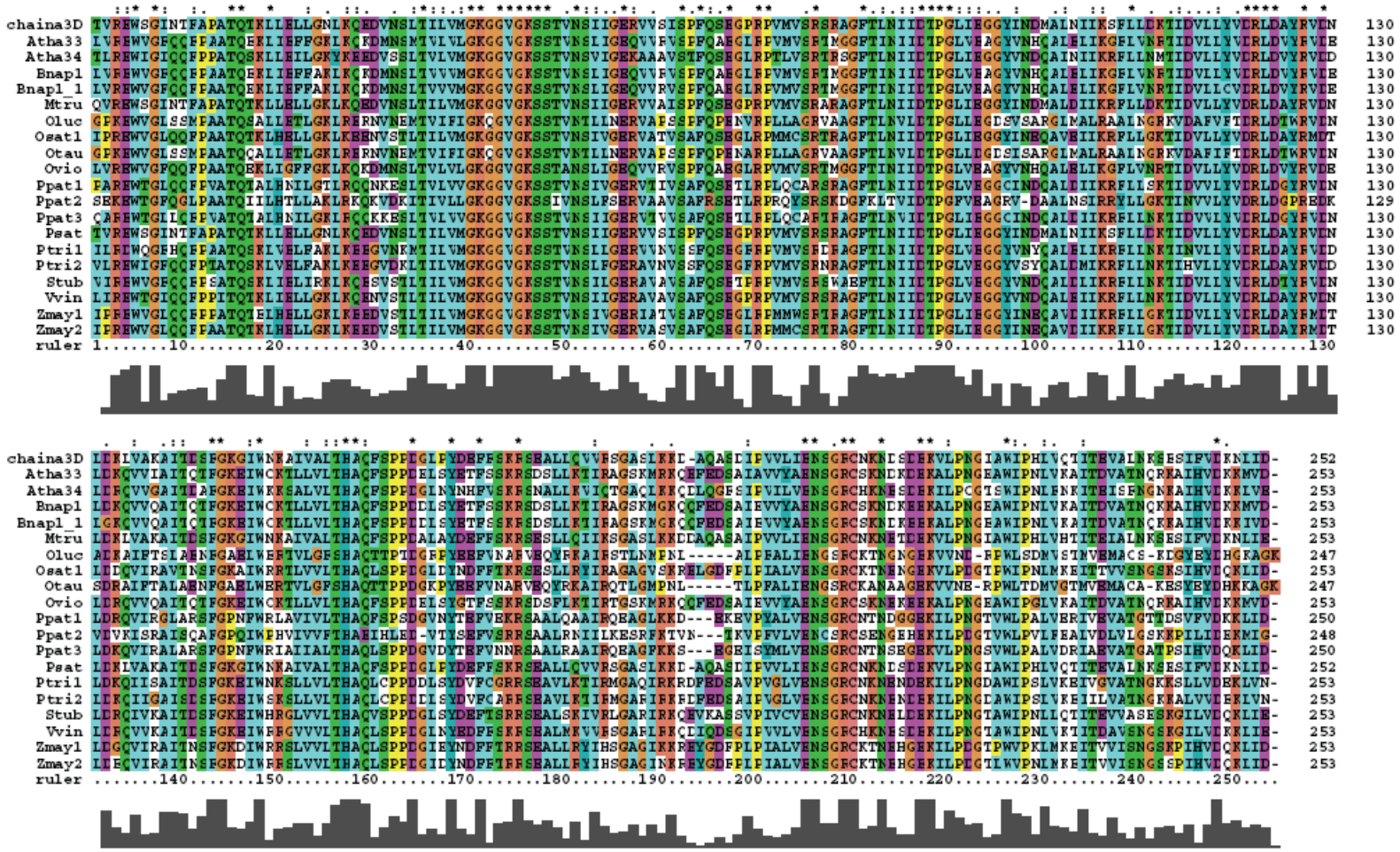

Figure S7. Alignment of Toc34 GTPases Used for Conservation Mapping as Shown in Figure S6

Prepared with ClustalX. The following proteins have been used in this alignment: Atha33: Toc33 from *Arabidopsis thaliana*, NP_171730; Atha34, Toc34 from *Arabidopsis thaliana*, NP_196119; Bnap1, Toc33 from *Brassica Nappus*, AAQ17548; Bnap1_1, TOC33-like protein from *Brassica Nappus*, AAQ73426; Mtru, Toc34 from *Medicago truncatula*, gb ABD28666.1; Oluc, predicted protein from *Ostreococcus lucimarinus CCE9901*, XP_001417009.1; Osat1, hypothetical protein OsJ_009702 from *Oryza sativa*, gb EAZ26219.1; Otau, Toc34 from *Ostreococcus tauri*, emb CAL53037.1; Ovio, Toc33-like protein from *Orychophragmus violaceus*, gb AAM77647.1; Ppat1, Toc34-1 from *Physcomitrella patens*, gb AAS47580.1; Ppat2, Toc34-2 from *Physcomitrella patens*, gb AAS47581.1; Ppat3, Toc34-3 from *Physcomitrella patens*, gb AAS47582.1; Psat, Toc34 from *Pisum sativum*, Q41009; Ptri1, protein from *Populus trichocarpa*, LG_XIV0229; Ptri2, protein from *Populus trichocarpa*, LG_II1667; Stub, GTP-binding-like protein from *Solanum tuberosum*, gb ABB16976.1; Vvin, hypothetical protein from *Vitis vinifera*, emb CAN63847.1; Zmay1, Toc34-1 protein from *Zea mays*, emb CAB65537.1; Zmay2, Toc34-2 protein from *Zea mays*, emb CAB77551.1.

Supplemental References

Glaser, F., Pupko, T., Paz, I., Bell, R.E., Bechor-Shental, D., Martz, E., and Ben-Tal, N. (2003). ConSurf: identification of functional regions in proteins by surface-mapping of phylogenetic information. Bioinformatics (Oxford, England) *19*, 163-164.

Krissinel, E., and Henrick, K. (2007). Inference of macromolecular assemblies from crystalline state. Journal of molecular biology *372*, 774-797.